



## UNITED STATES AIR FORCE RESEARCH LABORATORY

---

### An Analysis of the Response of Sooty Tern Eggs to Sonic Boom Overpressures

Carina Ting  
Joel Garrelick

CAMBRIDGE ACOUSTICAL ASSOCIATES, INC.  
200 Boston Avenue, Suite 2500  
Medford MA 02155-4243

Ann Bowles

HUBBS-SEA WORLD RESEARCH INSTITUTE  
2595 Ingraham Street  
San Diego CA 92109-7902

April 1997

Final Report for the Period March 1996 to April 1997

20011108 172

*Approved for public release; distribution is unlimited.*

Human Effectiveness Directorate  
Crew System Interface Division  
2610 Seventh Street  
Wright-Patterson AFB OH 45433-7901

## NOTICES

When US Government drawings, specifications, or other data are used for any purpose other than a definitely related Government procurement operation, the Government thereby incurs no responsibility nor any obligation whatsoever, and the fact that the Government may have formulated, furnished, or in any way supplied the said drawings, specifications, or other data, is not to be regarded by implication or otherwise, as in any manner licensing the holder or any other person or corporation, or conveying any rights or permission to manufacture, use, or sell any patented invention that may in any way be related thereto.

Please do not request copies of this report from the Air Force Research Laboratory. Additional copies may be purchased from:

National Technical Information Service  
5285 Port Royal Road  
Springfield, Virginia 22161

Federal Government agencies and their contractors registered with the Defense Technical Information Center should direct requests for copies of this report to:

Defense Technical Information Center  
8725 John J. Kingman Road, Suite 0944  
Ft. Belvoir, Virginia 22060-6218

## DISCLAIMER

This Technical Report is published as received and has not been edited by the Air Force Research Laboratory, Human Effectiveness Directorate.

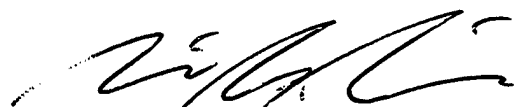
## TECHNICAL REVIEW AND APPROVAL

AFRL-HE-WP-TR-2001-0123

This report has been reviewed by the Office of Public Affairs (PA) and is releasable to the National Technical Information Service (NTIS). At NTIS, it will be available to the general public.

This technical report has been reviewed and is approved for publication.

**FOR THE COMMANDER**



MARIS M. VIKMANIS  
Chief, Crew System Interface Division  
Air Force Research Laboratory

REPORT DOCUMENTATION PAGE			Form Approved OMB No. 0704-0188	
Public reporting burden for this collection of information is estimated to average 1 hour per response, including the time for reviewing instructions, searching existing data sources, gathering and maintaining the data needed, and completing and reviewing the collection of information. Send comments regarding this burden estimate or any other aspect of this collection of information, including suggestions for reducing this burden, to Washington Headquarters Services, Directorate for Information Operations and Reports, 1215 Jefferson Davis Highway, Suite 1204, Arlington, VA 22202-4302, and to the Office of Management and Budget, Paperwork Reduction Project (0704-0188), Washington, DC 20503.				
1. AGENCY USE ONLY (Leave blank)		2. REPORT DATE April 1997		3. REPORT TYPE AND DATES COVERED Final - March 1996 to April 1997
4. TITLE AND SUBTITLE  An Analysis of the Response of Sooty Tern Eggs to Sonic Boom Overpressures			5. FUNDING NUMBERS C- F41624-96-C-9006 PE - 63723F PR - 2103 TA - 2103C2 WU - 2103C2D1	
6. AUTHOR(S)  Carina Ting, Joel Garrelick, Ann Bowles				
7. PERFORMING ORGANIZATION NAME(S) AND ADDRESS(ES)  Cambridge Acoustical Associates, Inc.      Hubbs-Sea World Research Institute 200 Boston Avenue, Suite 2500              2595 Ingraham Street Medford MA 02155-4243                      San Diego CA 92109-7902			8. PERFORMING ORGANIZATION REPORT NUMBER	
9. SPONSORING/MONITORING AGENCY NAME(S) AND ADDRESS(ES) Air Force Research Laboratory, Human Effectiveness Directorate Crew System Interface Division Aural Displays and Bioacoustics Branch Air Force Materiel Command Wright-Patterson AFB OH 45433-7901			10. SPONSORING/MONITORING AGENCY REPORT NUMBER  AFRL-HE-WP-TR-2001-0123	
11. SUPPLEMENTARY NOTES				
12a. DISTRIBUTION AVAILABILITY STATEMENT  Approved for public release; distribution is unlimited.			12b. DISTRIBUTION CODE	
13. ABSTRACT (Maximum 200 words) It has been suggested that sonic booms caused a mass hatching failure of Sooty Terns on the Dry Tortugas, Florida. Notwithstanding that the evidence was circumstantial, this hypothesis is often quoted as proof that sonic booms harm wildlife. The mathematical analysis reported herein is performed at two levels of idealization. The first model is that of a spherical elastic shell with the embryo represented as an inertial concentric sphere and the albumen as an acoustic fluid that completely fills the intervening volume. The second, higher fidelity, model accounts for the "egg shape" and allows for an air sac. In both cases the sonic boom is taken to be an incident acoustic wave with the classic N-wave signature. The peak responses of the egg, specifically the peak shell stress, embryo acceleration, and reactive force at the substrate upon which the egg rests, are computed as a function of the incident sonic boom overpressure and compared with damage criteria taken from the literature. It is concluded that the overpressures from supersonic military operations with existing aircraft are of insufficient level to cause avian egg damage in general and the 1970 Sooty Tern hatching failure in particular.				
14. SUBJECT TERMS  acoustics, noise impact, sonic boom, threatened and endangered species, egg breakage			15. NUMBER OF PAGES 46	
			16. PRICE CODE	
17. SECURITY CLASSIFICATION OF REPORT  UNCLASSIFIED	18. SECURITY CLASSIFICATION OF THIS PAGE  UNCLASSIFIED	19. SECURITY CLASSIFICATION OF ABSTRACT  UNCLASSIFIED	20. LIMITATION OF ABSTRACT  UL	

This page intentionally left blank.

## PREFACE

The work reported herein was conducted by Cambridge Acoustical Associates, Inc. of Medford MA from March 1996 to April 1997, under US Air Force contract F41624-96-C-9006. The government project number was 2103C2D1, and the contract monitor was Robert A. Lee of the Air Force Research Laboratory, Aural Displays and Bioacoustics Branch.

This page intentionally left blank.

## TABLE OF CONTENTS

I.	SUMMARY .....	1
II.	ANALYSIS .....	1
	A. Analytical Model of Spherically Symmetric Egg .....	3
	B. Numerical Model With Complex Egg Geometry .....	8
III.	NUMERICAL RESULTS .....	9
	A. Model Input Parameters .....	9
	B. Egg Failure Criteria .....	12
	C. Response Predictions .....	13
	D. Conclusions .....	17
	REFERENCES .....	19-20
	FIGURES .....	21-31
	APPENDIX A .....	A.1
	APPENDIX B .....	B.1
	FIGURE B.1 .....	B.3

This page intentionally left blank.



## I. SUMMARY

It has been suggested that sonic booms caused a mass hatching failure of Sooty Terns on the Dry Tortugas, Florida [1]. Notwithstanding that the evidence was circumstantial this hypothesis is often quoted as proof that sonic booms harm wildlife [2]. Although subsequent empirical studies with sonic boom-like impulsive noise sources have indicated that this thesis is unlikely [2,3] to date no complementary analytical study has been performed in their support. This study fills that gap by providing a mathematical analysis of the problem of avian eggs subjected to sonic boom overpressures and interpreting response predictions in terms of egg damage potential.

The analysis is performed at two levels of idealization. The first model is that of a spherical elastic shell with the embryo represented as an inertial concentric sphere and the albumen as an acoustic fluid that completely fills the intervening volume. The second, higher fidelity, model accounts for the "egg shape" and allows for an air sac. In both cases the sonic boom is taken to be an incident acoustic wave with the classic N-wave signature. The peak responses of the egg, specifically the peak shell stress, embryo acceleration, and reactive force at the substrate upon which the egg rests, are computed as a function of the incident sonic boom overpressure and compared with damage criteria taken from the literature (Table 5). It is concluded that the overpressures from supersonic military operations with existing aircraft, are of insufficient level to cause avian egg damage in general, and the 1970 Sooty Tern hatching failure in particular.

## II. ANALYSIS

The basic geometry for our analysis is sketched in Fig. 1. A supersonic operation produces a sonic boom that impinges on an egg resting on an effectively rigid substrate, or baffle. The overpressure is modeled as a plane acoustic wave with the classic N-wave signature. It is incident on the egg and substrate with a propagation vector having an elevation angle measured from the vertical of  $\alpha = \sin^{-1}(1/M)$ . The local Mach number

$M=U/c$  with  $U$  the effective flight speed and  $c$  the local air sound speed. In equation form

$$P_{boom}(x,y,t) = \frac{N_o}{2} \left[ \left( 1 - 2 \frac{t'}{\tau} \right) U_s(t') + \left( 1 + 2 \frac{(t'-\tau)}{\tau} \right) U_s(t'-\tau) \right] ,$$

$$t' = t - \frac{1}{c_o} [x \sin(\alpha) - y \cos(\alpha)] , \quad (1)$$

with the Fourier spectrum (transform) given by

$$\tilde{P}_{boom}(x,y,\omega) = \tilde{N}(\omega) \cdot P_{plane}(x,y,\alpha,\omega)$$

$$\tilde{N}(\omega) = \frac{N_o}{2} \left[ \frac{i}{\omega} [1 + \exp(i\omega\tau)] + \frac{2}{\tau\omega^2} [1 - \exp(i\omega\tau)] \right]$$

$$\tilde{P}_{plane}(x,y,\alpha,\omega) = \exp[+ik(x\sin(\alpha) - y\cos(\alpha))] . \quad (2)$$

In the above, we have assumed the harmonic time variation  $\exp(-i\omega t)$ , with time  $t$  and radial frequency  $\omega$ . The variable  $k = \omega/c$  is the acoustic wavenumber and  $\tau$  is the duration of the sonic boom.  $N_o$  represents the peak overpressure as typically measured, that is at ground level assuming pressure doubling.

Two levels of idealization are employed for the egg. In both cases the egg is treated as a linear system of continued and lumped elements. In one case however, its geometry is taken to be spherically symmetric and thus separable, allowing for closed form response predictions of shell stresses and embryo accelerations. This model, which turns out to be quite insightful, is presented below in Section A. A more detailed, numerical, model that explores the asymmetric influences of the egg shape and air sac characteristic of avian eggs, is presented in Section B.

### A. Analytical Model Of Spherically Symmetric Egg

This model is sketched in Fig. 2. The shell is treated as a thin, elastic, spherical shell of radius  $a$  and constant thickness  $h_s$ , and the embryo as a rigid inertial sphere of radius  $d$  and mass  $M_y$ , concentric with the shell. The albumen is represented by an acoustic fluid, of mass density  $\rho_a$  and sound speed  $c_a$ , that completely fills the intervening volume. See Fig. 2 for a sketch of the model dimensions and coordinate system. Here for the sake of simplicity, we maintain axisymmetry by considering only  $\alpha = 0$  or equivalently  $M \gg 1$ , i.e., high Mach number flights.

The rigid substrate upon which the egg rests is assumed to have two effects. It doubles the incident pressure over the egg surface, and it generates a reactive force that constrains the radial motion of the shell to be zero at  $\theta = 0$ . This force,  $F_R(\omega)$ , is taken to be the resultant of a uniformly distributed pressure over the assumed circular contact area,  $A_R = \pi a^2 \Delta^2$ , where  $\Delta$  is one-half the subtended polar angle. The solution to this problem is described below. Response function expressions,  $\tilde{f}(\omega)$ , are obtained in the frequency domain and, in turn, response time histories are computed by numerically taking their inverse Fourier transforms,

$$f(t) = \pi^{-1} \text{Re} \left[ \int_0^{\infty} \tilde{f}(\omega) \exp(-i\omega t) d\omega \right] .$$

The harmonic equations of motion of a thin, isotropic, axisymmetric spherical shell driven by the total radial pressure applied to the shell  $\tilde{p}(\theta, \omega)$ , may be expressed as [4]

$$\begin{aligned} \tilde{v}(\theta, \omega) &= \sum_{n=0}^{\infty} V_n \frac{d}{d\theta} P_n(\cos \theta) \\ \tilde{w}(\theta, \omega) &= \sum_{n=0}^{\infty} W_n P_n(\cos \theta) \end{aligned} \quad (3)$$

where the modal amplitudes  $V_n$  and  $W_n$  are given by the coupled equations

$$\begin{bmatrix} V_n \\ W_n \end{bmatrix} = \frac{-(1 - v_s^2)a^2}{E_s h_s} \begin{bmatrix} a_{11} & a_{12} \\ a_{21} & a_{22} \end{bmatrix}^{-1} \begin{bmatrix} 0 \\ P_n \end{bmatrix}$$

with

$$\begin{aligned} a_{11} &= \Omega^2 - (1 + \beta^2)(v_s + \lambda - 1) \\ a_{12} &= \beta^2(1 - v_s - \lambda) - (1 + v_s) \\ a_{21} &= -\lambda[\beta^2(v_s + \lambda - 1) + (1 + v_s)] \\ a_{22} &= \Omega^2 - 2(1 + v_s) - \beta^2\lambda(v_s + \lambda - 1) \\ \Omega &= \omega a \sqrt{\frac{\rho_s(1 - v_s^2)}{E_s}}, \quad \beta = \frac{h_s}{a\sqrt{12}}, \quad \lambda = n(n + 1) \end{aligned} \quad (4)$$

and

$$P_n = [(2n + 1)/2] \int_{-1}^1 \tilde{p}(\theta, \omega) P_n(\cos\theta) d(\cos\theta)$$

where  $E_s$  is Young's modulus and  $v_s$  Poisson's ratio of the shell material,  $\rho_s$  its mass density, and  $P_n()$  is the Legendre polynomial of order  $n$ . Vibration damping is provided by introducing the complex elastic modulus  $E_s \Rightarrow E_s(1 - i\eta_s)$  with  $\eta_s$  the structural loss factor. The dependent variables  $\tilde{v}$  and  $\tilde{w}$ , functions of the polar angle  $\theta$ , are the tangential and radial displacement components of the shell. These equations include both membrane and bending stresses, the latter represented by the  $\beta^2$  terms.

The total radial pressure applied to the shell consists of the external surface pressure  $\tilde{p}_s(\theta, \omega)$ , the internal pressure exerted by the albumen,  $\tilde{p}_a(\theta, \omega)$ , and the reactive pressure from the substrate interface,  $\tilde{p}_R(\theta, \omega)$

$$\tilde{p}(\theta, \omega) = \tilde{p}_s(\theta, \omega) + \tilde{p}_a(\theta, \omega) + \tilde{p}_R(\theta, \omega) \quad . \quad (5)$$

with

$$\begin{aligned} \tilde{p}_R(\theta, \omega) &= \tilde{F}_R(\omega)/A_R & \theta < \Delta \\ &= 0 & \text{otherwise} \end{aligned}$$

Ignoring sound radiation from the surrounding air, the modal amplitudes of the external pressure exerted on the sphere which is twice the incident pressure as given in Eq. 2, is [5].

$$(p_s)_n = \frac{2i}{(ka)^2} \frac{(2n+1)i^n}{h'_n(ka)} \tilde{N}(\omega) \quad , \quad (6)$$

where  $h'_n()$  is the derivative with respect to the argument of the spherical Hankel function of the first kind of order  $n$ .

The albumen being modeled as an acoustic fluid, the internal pressure is governed by the acoustic wave equation. The modal component of the force exerted on the shell by the internal fluid may be written as

$$(\tilde{p}_a(r))_n = -i\omega Z_n(r, \omega) W_n, \quad a > r > d \quad , \quad (7)$$

where the modal impedance  $Z_n$  has a solution of the form

$$Z_n(r, \omega) = a_n j_n(k_a r) + b_n y_n(k_a r) \quad , \quad (8)$$

where  $j_n()$  and  $y_n()$  are spherical Bessel functions of order  $n$ , of the first and second kind, respectively, and  $k_a = \omega/c_a$ . The modal coefficients  $a_n$  and  $b_n$  are defined by enforcing continuity with the radial displacement of the shell at  $r=a$  and with the rigid

spherical mass at  $r=d$ . The solution is

$$\begin{bmatrix} a_n \\ b_n \end{bmatrix} = \begin{bmatrix} j_n'(k_i d) & y_n'(k_i d) \\ (j_n'(k_i d) - i \rho_i c_i j_n(k_i d) Y_n) & (y_n'(k_i d) - i \rho_i c_i y_n(k_i d) Y_n) \end{bmatrix}^{-1} \begin{bmatrix} i \rho_i c_i \\ 0 \end{bmatrix}, \quad (9)$$

where  $Y_n$  is the translational admittance of the mass, given as

$$\begin{aligned} Y_{n=1} &= -i \frac{4\pi d^2}{3\omega M_y} \\ Y_{n \neq 1} &= 0 \end{aligned} \quad (10)$$

with  $M_y = \rho_y \frac{4}{3} \pi d^3$  where  $\rho_y$  is the yolk mass density. To obtain the modal coefficients of the internal surface pressure on the shell, Eq. 7 is evaluated at  $r=a$ .

The modal coefficients for the interface pressure are obtained from the integral expression in Eq. 4 as

$$(p_R)_n = \frac{(2n+1)F_R(\omega)/A_R}{2(n+1)} [P_{n-1}(\cos(\Delta)) - \cos(\Delta)P_n(\cos(\Delta))] \quad (11)$$

It remains to solve for the value of  $\tilde{F}_R(\omega)/A_R$  that enforces the boundary condition

$$\tilde{w}(\theta=0, \omega) = 0 \quad (12)$$

Using equations (4), (7), (11) and (12) of this reaction force becomes

$$(F_R(\omega)/A_R) = - \frac{\sum_{n=0}^{\infty} \frac{a_{12}(p_s)_n}{\bar{D}}}{\sum_{n=0}^{\infty} \frac{a_{12}(p_R)_n}{\bar{D}}}$$

with

$$\bar{D} = a_{11} a_{22} - a_{12} \left( a_{21} - \frac{i\omega (1-v_s^2) a^2}{E_s h_s} Z_n(r=a, \omega) \right) \quad (13)$$

The solution for the shell displacements may now be obtained via substitution of Eqs. (6), (7) and (13) into equations (4) and (5). The associated shell stresses are completely defined by these displacements. Using conventional notation, these stresses are given by [6]

$$\begin{aligned} \tilde{\sigma}_\theta(z, \theta, \omega) = \frac{E_s}{(1-v_s^2)a} & \left[ \left[ (1+v_s) - \frac{z}{a} \left( \frac{\partial^2}{\partial \theta^2} + v_s \cot(\theta) \frac{\partial}{\partial \theta} \right) \right] \tilde{w}(\theta, \omega) + \right. \\ & \left. \left[ \frac{\partial}{\partial \theta} + v_s \cot(\theta) - \frac{z}{a} \left( \frac{\partial}{\partial \theta} + v_s \cot(\theta) \right) \right] \tilde{v}(\theta, \omega) \right] , \end{aligned} \quad (14)$$

$$\begin{aligned} \tilde{\sigma}_\phi(z, \theta, \omega) = \frac{E_s}{(1-v_s^2)a} & \left[ \left[ (1+v_s) - \frac{z}{a} \left( v_s \frac{\partial^2}{\partial \theta^2} + \cot(\theta) \frac{\partial}{\partial \theta} \right) \right] \tilde{w}(\theta, \omega) + \right. \\ & \left. \left[ v_s \frac{\partial}{\partial \theta} + \cot(\theta) - \frac{z}{a} \left( v_s \frac{\partial}{\partial \theta} + \cot(\theta) \right) \right] \tilde{v}(\theta, \omega) \right] , \end{aligned} \quad (15)$$

$$\begin{aligned} \tilde{\tau}_{\theta z}(z, \theta, \omega) = & \frac{E_s h_s^2}{8(1 - \nu_s^2) a^3} \left( 1 - \left( \frac{z}{h} \right)^2 \right) \cdot \\ & \left[ \left[ \frac{\partial^3}{\partial \theta^3} + \cot(\theta) \frac{\partial^2}{\partial \theta^2} - (1 - \nu_s) \cot^2(\theta) \frac{\partial}{\partial \theta} \right] \tilde{w}(\theta, \omega) + \right. \\ & \left. \left[ \frac{\partial^2}{\partial \theta^2} + \cot(\theta) \frac{\partial}{\partial \theta} - (1 - \nu_s) \cot^2(\theta) \right] \tilde{v}(\theta, \omega) \right] \cdot \quad (16) \end{aligned}$$

where  $z$  is the distance from the neutral axis of the shell.

Finally, the vertical embryo acceleration becomes

$$\ddot{\Xi} = - \omega^2 Z_a^{n=1}(r=d, \omega) Y_{n=1} W_{n=1} \quad (17)$$

### B. Numerical Model With Complex Egg Geometry

With this model, the geometry of the egg shell is treated with greater geometric fidelity and the air sac is represented. It is sketched in Fig. 3. The shell is again modeled as thin and linearly elastic, and capable of both membrane and flexural stresses. However here the embryo and air sac, as well as the albumen, are modeled as acoustic media. The model was solved numerically, using finite elements. The egg shell is developed from bending and membrane plate elements. Consistent with Ref. 7, the shell geometry is characterized as a composite ellipsoid described by



$$\begin{aligned}
r' &= \frac{B}{2} \left[ 1 - \left( \frac{z'}{D} \right)^2 \right]^{\frac{1}{2}}, \quad -D < z' < 0 \\
r' &= \frac{B}{2} \left[ 1 - \left( \frac{z'}{L-D} \right)^2 \right]^{\frac{1}{2}}, \quad 0 < z' < L-D \\
0 < \theta' < 2\pi
\end{aligned} \tag{18}$$

where  $r'$ ,  $z'$ , and  $\theta'$  are cylindrical coordinates,  $L$  is the length of the axis of the egg,  $B$  is the largest diameter perpendicular to the axis and  $D$  is the distance from the largest diameter to the blunt side of the egg along the axis (Fig. 3). Acoustic fluid elements represent the albumen, egg yolk and air sac [8]. It was implemented using Cosmic Nastran Finite Element Analysis Software. Our finite element mesh is shown in Fig. 4.

The egg is positioned on the substrate so that the height of its center of mass is minimized. The substrate itself is again taken to be rigid and as before radiation loading is ignored. However, rather than simply doubling the incident pressure on the egg surface as was done for the analytical model, here the surface pressure was actually computed for a plane wave incident on the egg in the presence of the rigid planar boundary, using the computer code Nashua [9]. The elastic egg is constrained such that there are zero shell displacements at the single shell-substrate interface node. We again interpret the reaction force to be a uniformly distributed pressure, now acting over the average of the areas of the elements adjacent to the constrained node. The response is obtained using Cosmic Nastran's direct frequency solution.

### III. NUMERICAL RESULTS

#### A. Model Input Parameters

In this section we describe the input parameters for our models. For a given air sound speed, the sonic boom, represented as an N-wave, is fully defined by the peak

pressure and duration. Further, since our models are linear, all response functions may be computed for a unit peak pressure and scaled accordingly. For the sonic boom duration, we take 0.15s, a representative value for U. S. Air Force fighter aircraft. Two incident elevation angles are considered,  $\alpha = 0^\circ$  and  $56^\circ$ , the latter simulating an overflight at roughly Mach 1.2. These parameters are summarized in Table 1.

**Table 1.** N-Wave Sonic Boom Excitation Parameters

Description	Symbol	Value(s)
Air Speed of Sound	$c$	330 m / s
Sonic Boom Amplitude	$N_o$	1 Pa
Sonic Boom Duration	$\tau$	0.15 s
Incident Angle (Mach Number)	$\alpha$	$0^\circ, 56^\circ (\infty, 1.2)$

Published data [10] indicate that the basic structure and dimensions for eggs of a variety of bird species, including the sooty tern, are similar to those of common chicken eggs, for which there are a number of published sources of measured physical properties. Accordingly, the material property and geometric parameters that we have chosen for our study, and that are summarized in Tables 2 and 3, are based on chicken egg data.

**Table 2.** Material Properties for Egg Models.

Description	Symbol	Value
Shell Elastic Modulus	$E_s$	$1.1 \cdot 10^{11} \text{ Pa}$
Shell Poisson's Ratio	$\nu_s$	0.3
Shell Mass Density	$\rho_s$	$2000 \text{ kg / m}^3$
Shell Loss Factor	$\eta_s$	0.01
Albumen Mass Density	$\rho_a$	$1000 \text{ kg / m}^3$
Albumen Speed of Sound	$c_a$	$1500 \text{ m / s}$
Yolk Mass Density	$\rho_y$	$1100 \text{ kg / m}^3$
Yolk	$c_y$	$1500 \text{ m / s}$

The elastic modulus of the shell is subject to considerable uncertainty, with values in the literature ranging from  $1 \times 10^{10}$  to  $20 \times 10^{10} \text{ Pa}$  [11,12]. The value chosen, which falls within this range, is consistent with values computed from ultrasonic measurements of the compressional wave speed in a chicken egg shell that were commissioned for this study ( $c_s = 6,900 \text{ m/s}$ ), and the listed shell density,  $E_s = \rho_s c_s^2$ . (See Appendix A.) The mass densities were estimated from measurements performed on purchased chicken eggs. The speed of sound of the egg white and that of the yolk were taken from [13]. We interpret a chick embryo to have similar physical properties to a yolk. The shell loss factor, for which no data could be found, was chosen somewhat arbitrarily. Dimensions were estimated from measurements using chicken eggs. The shell thickness listed, which was measured at the thinnest part of the shell, is consistent with other published sources [7,12]. The values of L, B, and D agree with those in Ref. 7.

**Table 3.** Egg Dimensions

Description	Symbol	Value
Thickness of Shell	$h_s$	3.6 mm
Length of Shell	L	5.7 cm
Largest Breadth of Shell	B	4.2 cm
Distance from Largest Breadth to Blunt End of Egg	D	2.5 cm
Radius of Spherical Shell	a	2.3 cm
Radius of Yolk/Embryo	d	1.5 cm
Area of Contact	$A_R$	0.15 cm <sup>2</sup>

For our spherical model, the radius  $a$  was chosen by equating egg volumes. For the finite element model, the shell interface area over which the substrate reaction is spread was conservatively chosen to be considerably less than that measured with a chicken egg resting on compacted sand (7.7 cm<sup>2</sup>), while at the same time computationally convenient.

#### **B. Egg Failure Criteria**

Peak egg shell stress and peak embryo acceleration are chosen as our primary damage metrics. Corresponding failure criteria, that is maximum allowable levels, are shown in Table 4. As with its elastic modulus, there is a good deal of spread in the published data for the ultimate egg shell stress. To err on the conservative side, the value of  $1.2 \times 10^7$  Pa shown in Table 4 is the lowest reported in Ref. 11, where values between  $1.2 \times 10^7$  and  $5.6 \times 10^7$  Pa are presented. The maximum embryo acceleration listed is taken from Ref. 14. In this reference, experiments are described that indicate egg yolks subjected to the listed acceleration over a 1.5 ms period, yield no damage on the

cellular level. The duration is appropriate, since as will be seen, the computed embryo acceleration is a damped oscillatory motion with a period on the order of 1. ms.

Finally, as a result of our study, a third failure criterion is proposed in Table 4. It is the maximum allowable concentrated radial force that may be applied to the egg. During egg shell failure tests conducted as part of this study by the Department of Plastics Engineering at the University of Massachusetts at Lowell (Appendix B) it was found that egg failure correlated quite well with the force applied by the testing machine. It is therefore proposed as a more robust failure metric than ultimate stress. The value shown in Table 4 should be conservative in that during these tests, the eggs were placed between rigid platens, thus minimizing the area of contact and in turn maximizing the stress.

**Table 4.** Egg Failure Criteria

Description	Value
Ultimate Stress of Shell	$1.2 \cdot 10^7$ Pa
Maximum Embryo Acceleration	988 g (1.5 ms duration)
Force to Break Chicken Egg	3.2 N

### C. Response Predictions

In this section we present computed response predictions for both our analytical and numerical models. We focus on the maximum egg shell stress, specifically the flexural stress at the substrate interface ( $\sigma_\theta$  with  $z = h_s/2$  and  $\theta = 0$  in Eq. 14), which we find to predominate. The embryo acceleration,  $\Xi$ , and the substrate reactive force on the egg,  $F_R$  are also presented. All results are normalized to  $N_o$ , twice the value of the *free field* peak overpressure, to simulate the practice of referring to the strength of a sonic boom as that measured at ground level, as noted previously.

### 1. Analytical Model

Time histories computed for the shell stress, embryo acceleration and substrate reactive force are presented in Fig. 5. All three signatures suggest the response of a damped oscillator impulsively executed at  $t=0$  and  $t=0.15$  s, the initiation and termination times of the N-wave. (Although not readily apparent in Fig. 7, the oscillations correspond to a frequency of 1,040 Hz.) To pursue this notion further, consider the single degree of freedom, lumped parameter model illustrated in Fig. 6. For the mass,  $M$ , we take the total mass of the egg. The spring stiffness is estimated as the local stiffness of the spherical shell statically loaded by a uniform radial pressure over a circular cap of area,  $A_R \ll 2ah_s$  [15]

$$K \doteq \frac{E_s h_s^2}{a} \left[ 0.42 - 0.116 \frac{A_R}{ah_s} + 0.023 \left( \frac{A_R}{ah_s} \right)^2 \right]^{-1}, \quad (19a)$$

and the dashpot constant,  $B$  is estimated from the structural loss factor in the egg shell

$$B \doteq \eta_s \sqrt{KM} \quad . \quad (19b)$$

Assuming a small loss factor, this results in the natural frequency

$$\omega_o \doteq \sqrt{\frac{K}{M}} \quad . \quad (20)$$

For the parameters provided in Tables 1 and 2 we predict a natural frequency of 980 Hz, comparing favorably with the 1,040 Hz oscillations in Fig. 5.

Continuing with this simplified model, and assuming that the egg is small in terms of acoustic wavelength in air, that is  $ka \ll 1$ , the net translational force applied to the shell by twice the incident wave becomes

$$\tilde{F}_{egg}(\omega) \doteq i \omega \frac{2 \pi a^3}{c_o} 2\tilde{P}_{boom}(x=0, y=0, \omega) \quad , \quad (21)$$

and in turn

$$F_{egg}(t) \doteq \frac{2 \pi a^3}{c_o} \frac{d}{dt} (2P_{boom}(x=0, y=0, t)) \quad , \quad (22)$$

where the location (x, y) is arbitrarily chosen to be (0, 0). The solution to this forced problem is readily obtained. The reaction force, specifically the force stored in the spring, is given by

$$F_R(t) \doteq N_o \frac{2 \pi a^3 \omega}{c} \dot{c} \left[ \exp\left(-\frac{\eta_s}{2} \omega t\right) \sin(\omega t) + \exp\left(-\frac{\eta_s}{2} \omega (t - \tau)\right) \sin(\omega (t - \tau)) \right] \quad , \quad (23)$$

$$\omega_o a / c \ll 1, \quad \omega \tau \gg 1 \quad .$$

The associated maximum stress in a thin shell, subject to this reaction force is [15].

$$\sigma_\theta \left( z = \frac{h_s}{2}, \theta = 0 \right) \doteq \frac{F_R(t)}{h_s^2} \left[ 0.42 - 0.282 \ln \left( \frac{A_R}{a h_s} \right) \right] , \quad A_R < 2 a h_s \quad . \quad (24)$$

The corresponding acceleration of the mass (embryo) is

$$\Xi(t) \doteq N_o \frac{2\pi a^3 \omega}{M_{egg} c_o} \cdot \left[ \exp\left(-\frac{\eta_s}{2} \omega t\right) \sin(\omega t) + \exp\left(-\frac{\eta_s}{2} \omega(t-\tau)\right) \sin(\omega(t-\tau)) \right] ,$$

$$\omega_o a/c \ll 1, \omega_o \tau \gg 1 \quad . \quad (25)$$

Eqs. 23, 24 and 25 are plotted in Fig. 7 for comparison with their counterparts in Fig. 5. The agreement is good. For example, the difference between the computed peak stresses is only 17 %. This comparison is also reassuringly insightful in that the lumped parameter model shows explicitly that the peak amplitudes are insensitive to the exact choice of the loss factor, as long as it is small.

## 2. Numerical Model

Before computing response time histories with our numerical model, a modal analysis was performed. The cross-sectional shape of the fundamental mode is sketched in Fig. 8. Its natural frequency is 957 Hz. It appears that most of the egg mass translates as a rigid body with elastic deformation limited to the immediate vicinity of the substrate constraint. The air sac and yolk do not seem to play a significant role. These results are consistent with the lumped parameter model of the egg described earlier. To compare with the findings from our analytical model, we initially consider the case with  $\alpha = 0$ .

First for diagnostic purposes, we follow the approach taken in the previous section to represent the influence of the substrate. That is, we constrain the motion of the egg at the interface and double the incident pressure. These results are shown in Fig. 9. They are quite similar to our earlier predictions. The maximum shell stress is slightly larger than that in Fig. 5. This may be attributed to the larger radius of curvature at the interface. However, this picture changes with our complete numerical model. Here,



rather than a priori doubling the incident pressure we account fully for the diffractive and reflective effects of the substrate. These results are shown in Fig. 10, again with  $\alpha = 0$ . We note that now the peak levels are significantly lower and the time signatures more closely resemble the incident N-wave.

For insight into this outcome, we return to the simple lumped parameter model. The oscillator was driven by a net translational force produced by the  $n=1$  modal component of the incident pressure field evaluated on the shell surface. An assumed doubling of the pressure doubled the force. However, with normal incidence, the reflected wave from a rigid substrate propagates in the opposite direction. Consequently, it tends to cancel any net translation force, especially for small values of  $ka$ . In turn, response levels are reduced. The remaining modal components tend to produce local reaction or spring-like response, which mirrors the time signature of the incident wave. Finally, in Fig 11 we present results for the egg response to an incident sonic boom with  $\alpha = 56^\circ$  and note that predicted levels are roughly 50% lower than those in Fig.10.

#### **D. Conclusions**

The ramifications of our predictions on failure potential are summarized in Table 5. Specifically, we show in Table 5 the values of  $N_o$  that would be required for the predicted failure metrics (peak shell stress, egg acceleration and reaction force) to equal the failure values in Table 4. They are unreasonably high, especially in view of our consistent employment of conservative assumptions. For perspective, the "loudest" sonic boom recorded during a recent six month military exercise involving 385 supersonic sorties was 19.4 psf [16]. We therefore conclude sonic boom overpressures from supersonic aircraft operations are of insufficient levels to cause avian egg damage.

**Table 5.** Peak Sonic Boom Overpressure Required for Failure ( $\alpha = 0$ )

Failure Criterion	$N_o$ Required For Failure	
	Analytical Model, $P_a(psf)$	Numerical Model $P_a(psf)$
Maximum Shell Stress	$3.75 \times 10^3 (7.8 \times 10^1)$	$1.27 \times 10^4 (2.67 \times 10^2)$
Yolk Acceleration	$4.3 \times 10^5 (8.98 \times 10^3)$	$3.66 \times 10^6 (7.65 \times 10^4)$
Substrate Force	$2.46 \times 10^3 (5.1 \times 10^1)$	$1.19 \times 10^4 (2.48 \times 10^2)$

## REFERENCES

- 1 - Austin, O.L., Jr., et al., "Mass Hatching Failure in Dry Tortugas Sooty Terns", Proc. Int. Ornithological Cong. 15:627, 1970.
- 2 - Bowles, A.E., et al., "The Effects of High Amplitude impulsive noise on hatching success: a reanalysis of the sooty tern incident", Noise and Sonic boom Impact technology program, OL-AC HSD/YAH (NSBIT) Report # hsd-tp-91-0006, 1991.
- 3 - Bowles, A.E., et al., "Effects of Simulated Sonic Booms on the Hatchability of White Leghorn Chicken Eggs", Occupational and Environmental Health Directorate AL/OE-TR-1994-0179, 1994.
- 4 - Junger, M. C., Feit, D., Sound, Structures, and Their Interaction, The MIT Press, Cambridge, MA, 1972.
- 5 - Op cit. p. 319.
- 6 - Timoshenko, S. and Woinowsky-Krieger, S., Theory of Plates and Shells, McGraw-Hill Book Company, Inc., NY, 1959.
- 7 - Romanoff, A.L. and Romanoff, A.J., The Avian Egg, John Wiley and Sons, NY, 1969.
- 8 - Everstine, G.C., et. al., "Finite Element Prediction of Acoustic Scattering and Radiation from Submerged Elastic Structures", Nastran Users Colloquium, 1987.
- 9 - Everstine, G.C. and Henderson, F.M., "Coupled Finite Element / Boundary Element Approach for Fluid-Structure Interaction", J. Acoust. Soc. Am **87**, 1938-1947 (1990).
- 10 - Hoyt, D. F., "Practical Methods of Estimating Volume and Fresh Weight of Bird Eggs," The Auk **96**: 73-77 (1979).
- 11 - Voisy, P. W. and Hunt, J. R., "Review Paper: Measurement of Eggshell Strength", Journal of Texture Studies, **5** 135-182 (1974).
- 12 - Lin, J., et al, "Measurement of Eggshell Thermal-Mechanical Properties", Transactions of the ASAE, 00001-2351 /95/ 3806-1769, 1995.
- 13 - Javanaud, C., et al, "Measurement of speed and attenuation of ultrasound in egg white and egg yolk", J. Acoust. Soc. Am, **76** (3), 670-675, 1984.
- 14 - Besch, E.L. et al., "Morphological changes in avian eggs subjected to accelerative force", Journal of Applied Physiology **20** (6): 1241-1248, 1965.
- 15 - Roark, R. J., Formulas for Stress and Strain, McGraw-Hill Book Company, Inc, NY, 1954.

- 16 - Kenneth D. Frampton, Michael J. Lucas and Kenneth J. Plotkin, "Measurements of Sonic Booms Due to ACM Training in the Elgin MOA Subsection of the Nellis Range Complex," Wyle Research Report WR 93-5, prepared for Douglas Aircraft Company, (April 1993).

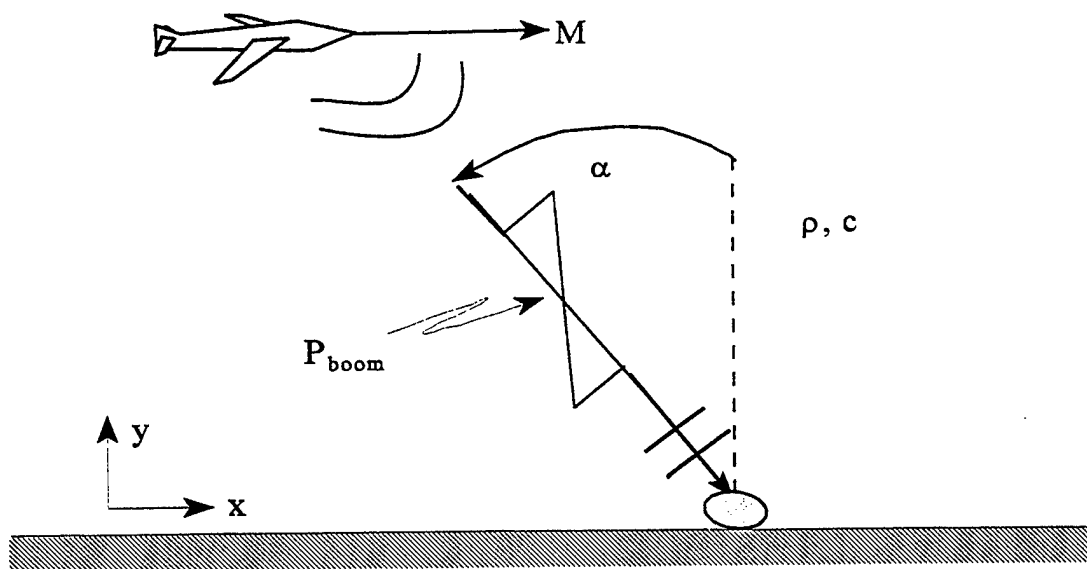
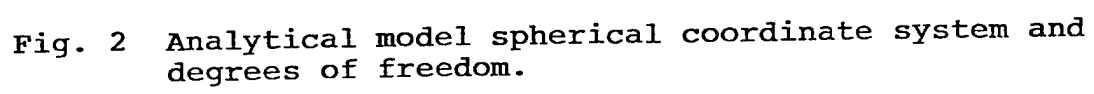


Fig. 1 Sonic boom model and coordinate system.



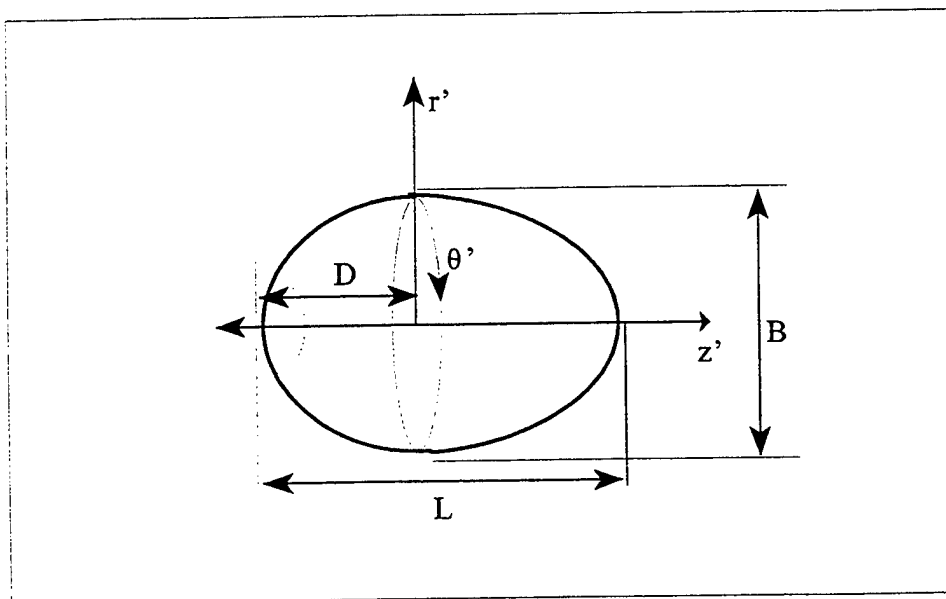
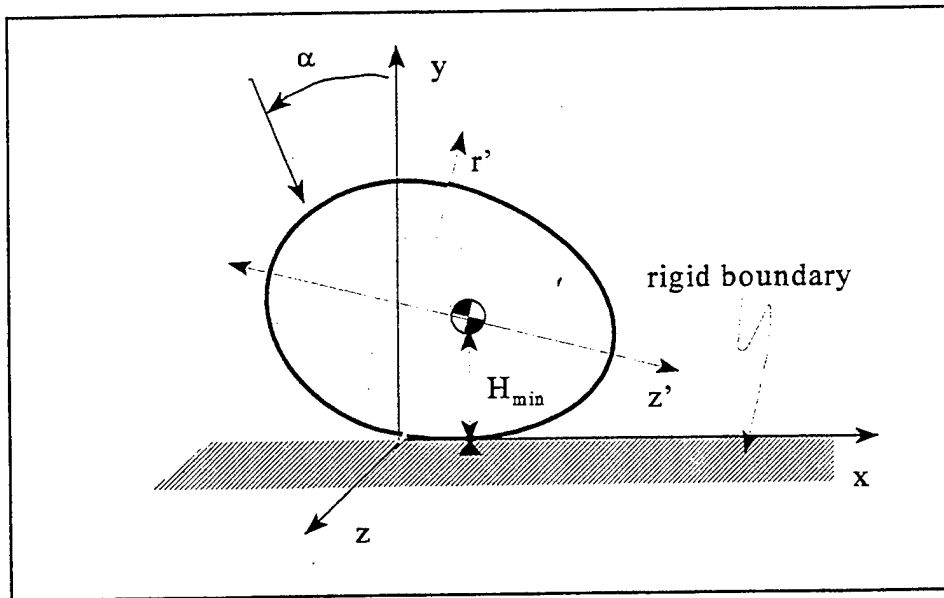


Fig. 3 Finite element model boundary conditions and orientation relative to rigid boundary.

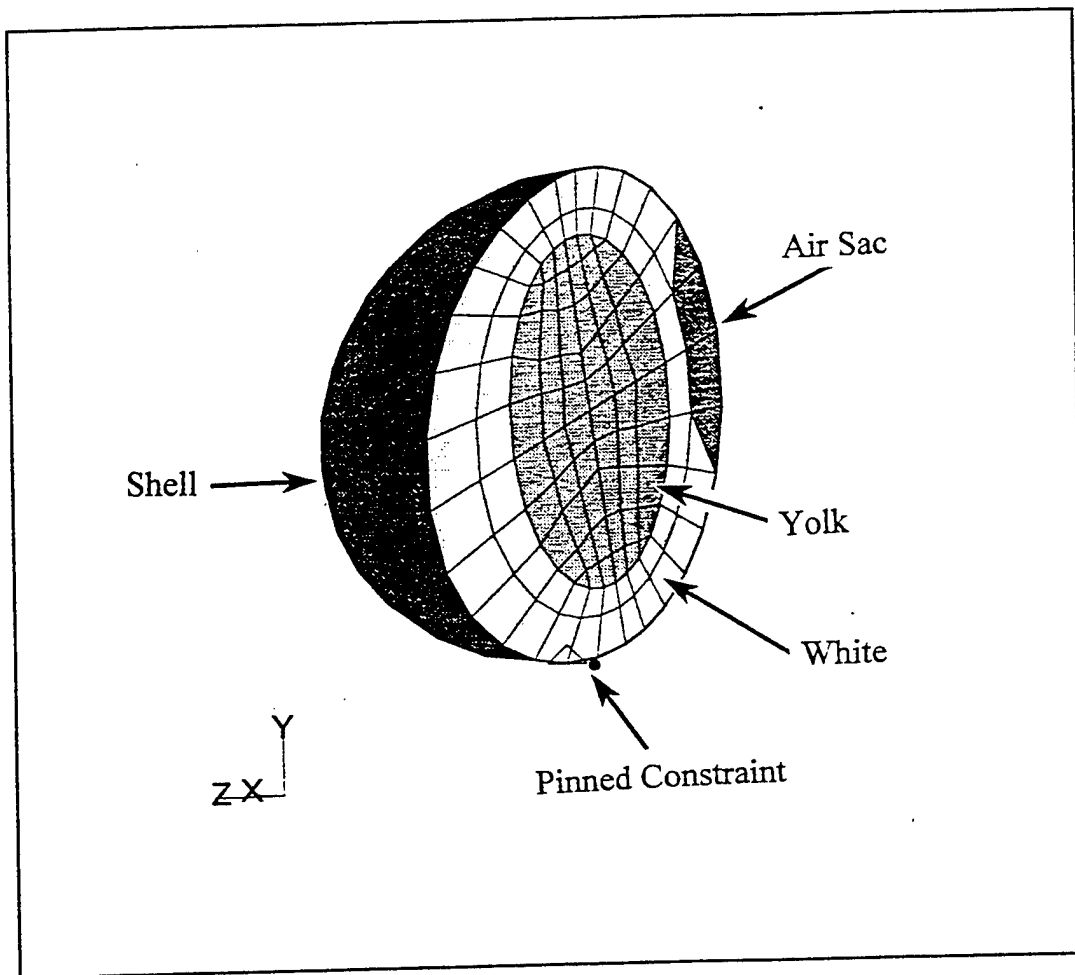


Fig. 4 Finite element mesh of egg.



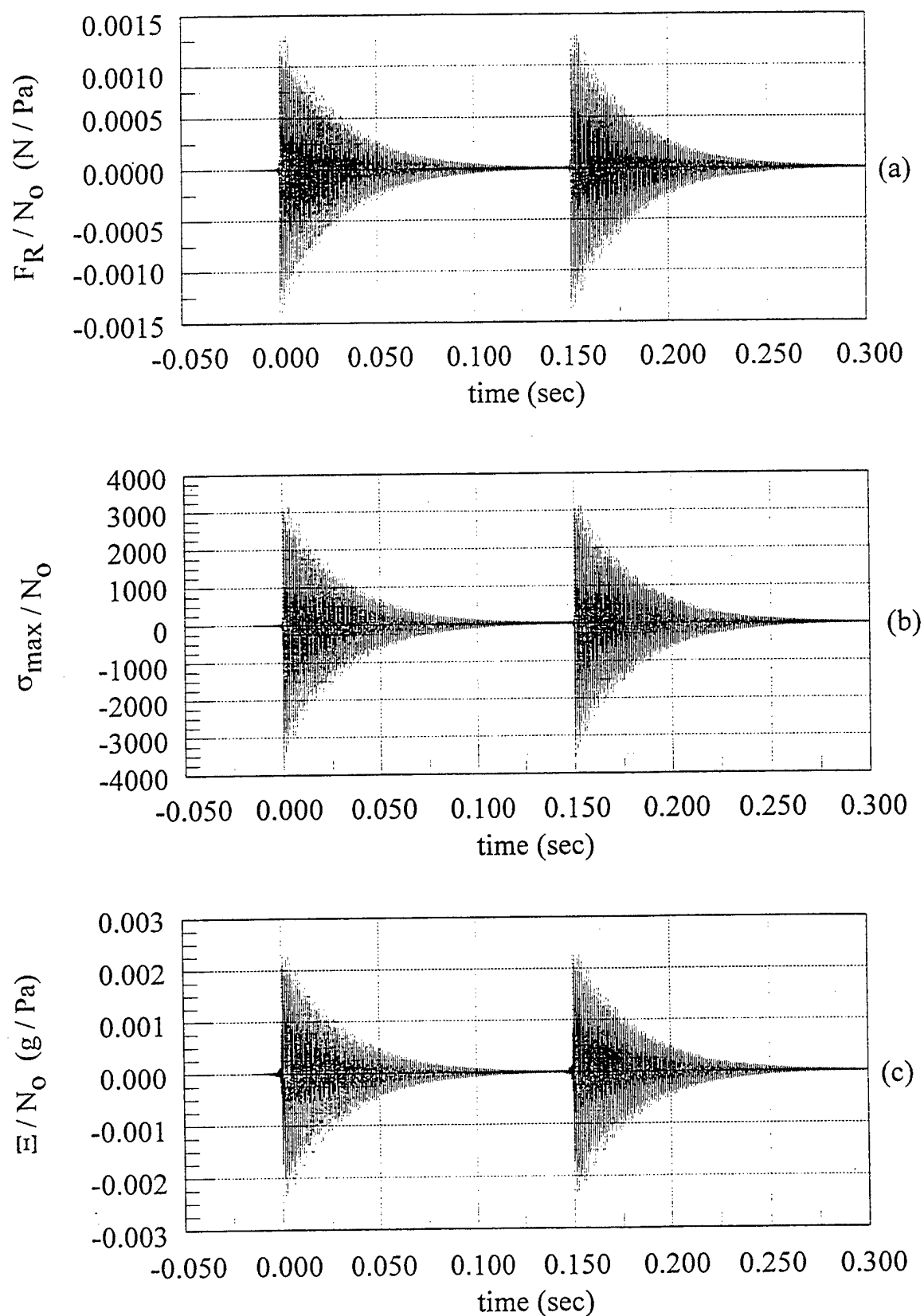


Fig. 5 Analytical model response to unit N-wave excitation at  $\alpha=0$ . (a) reaction force (b) stress at position of peak stress (c) embryo acceleration.

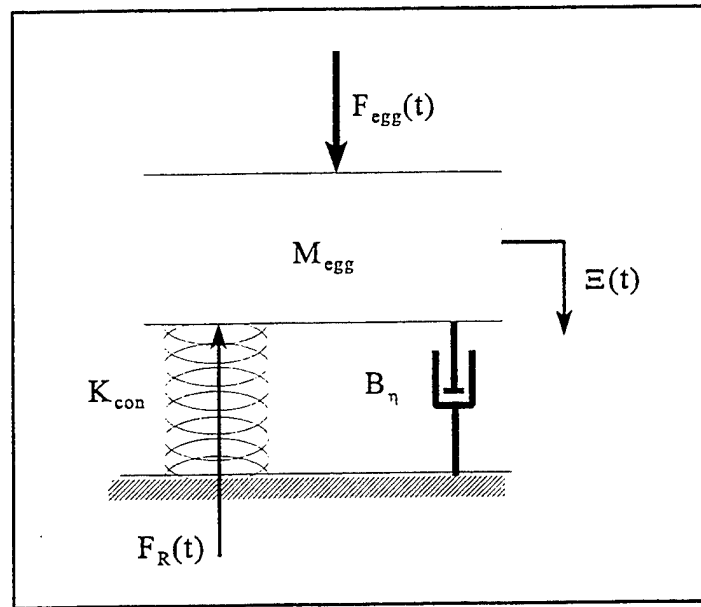


Fig. 6 Lumped parameter model of egg.

lumped

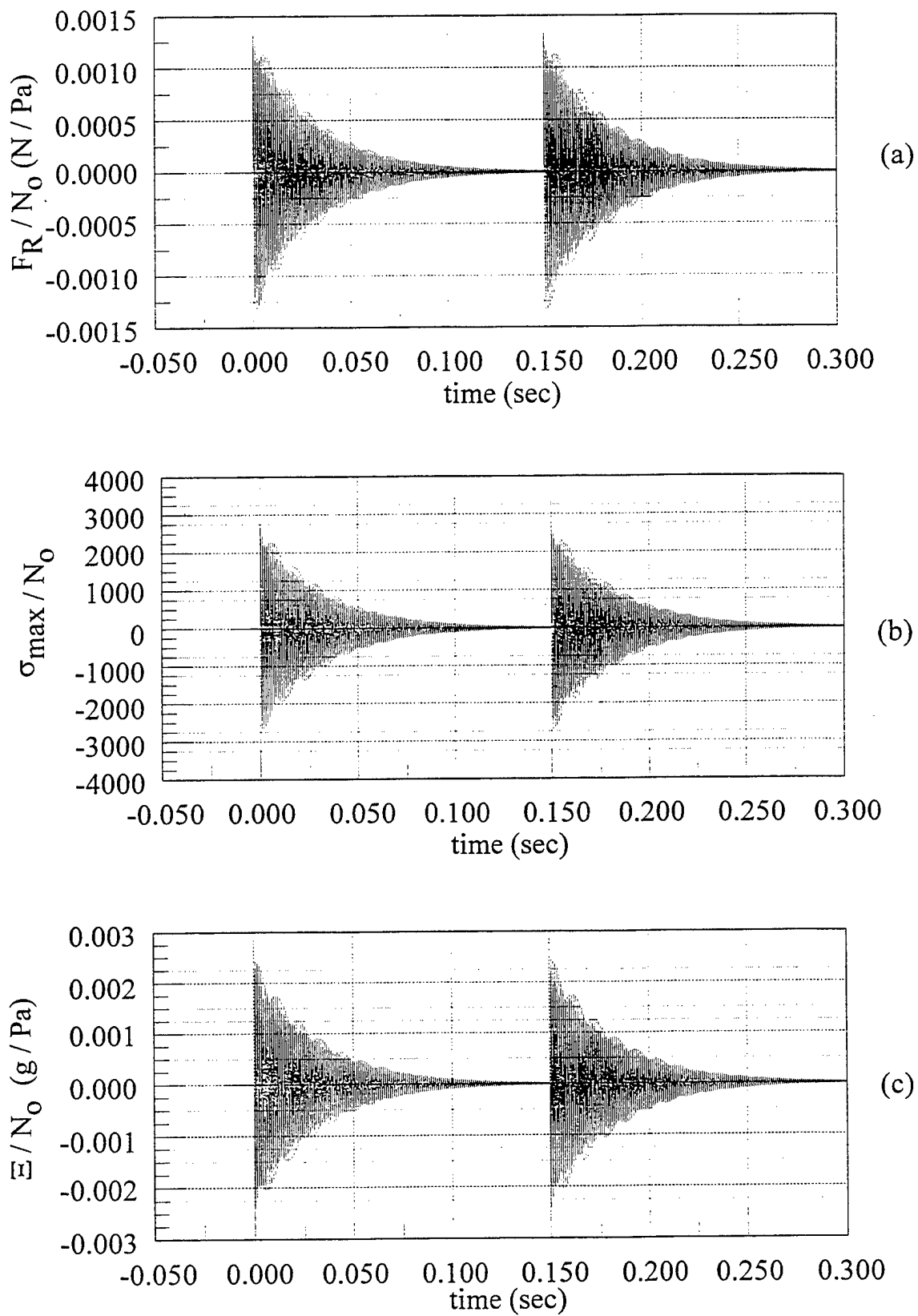


Fig. 7 Lumped parameter model response to unit N-wave excitation at  $\alpha=0$ . (a) reaction force (b) stress at position of peak stress (c) embryo acceleration.

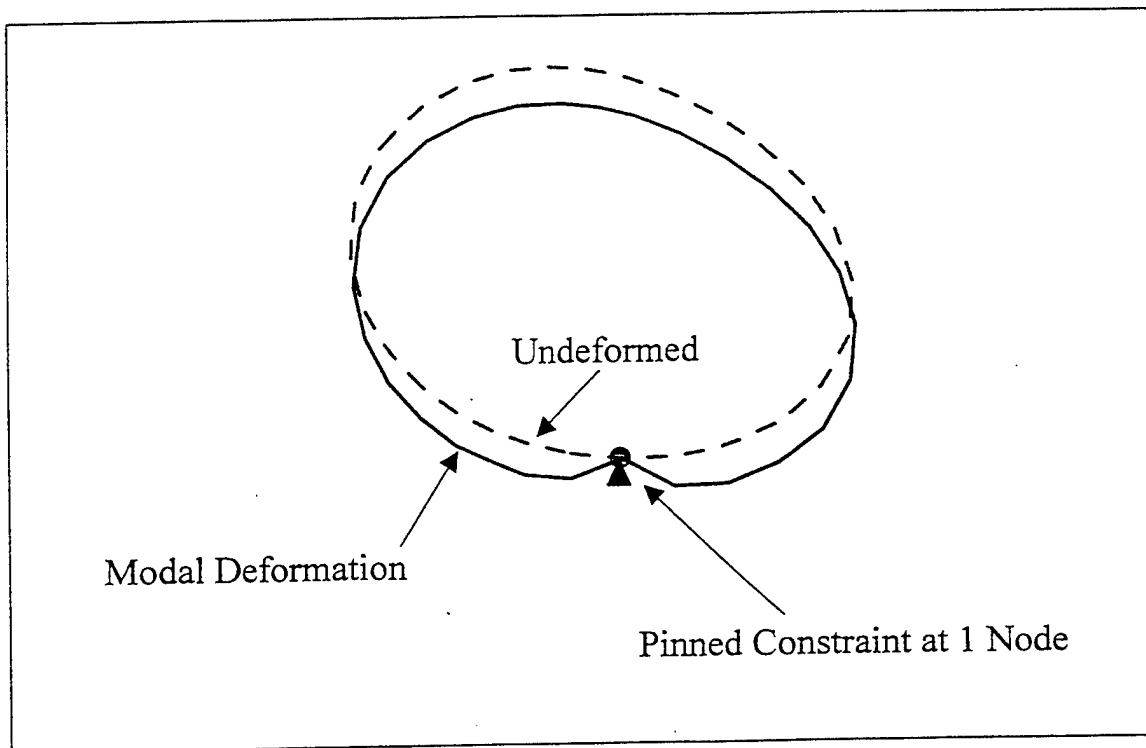


Fig. 8 Fundamental mode shape of egg shell at 957 Hz.

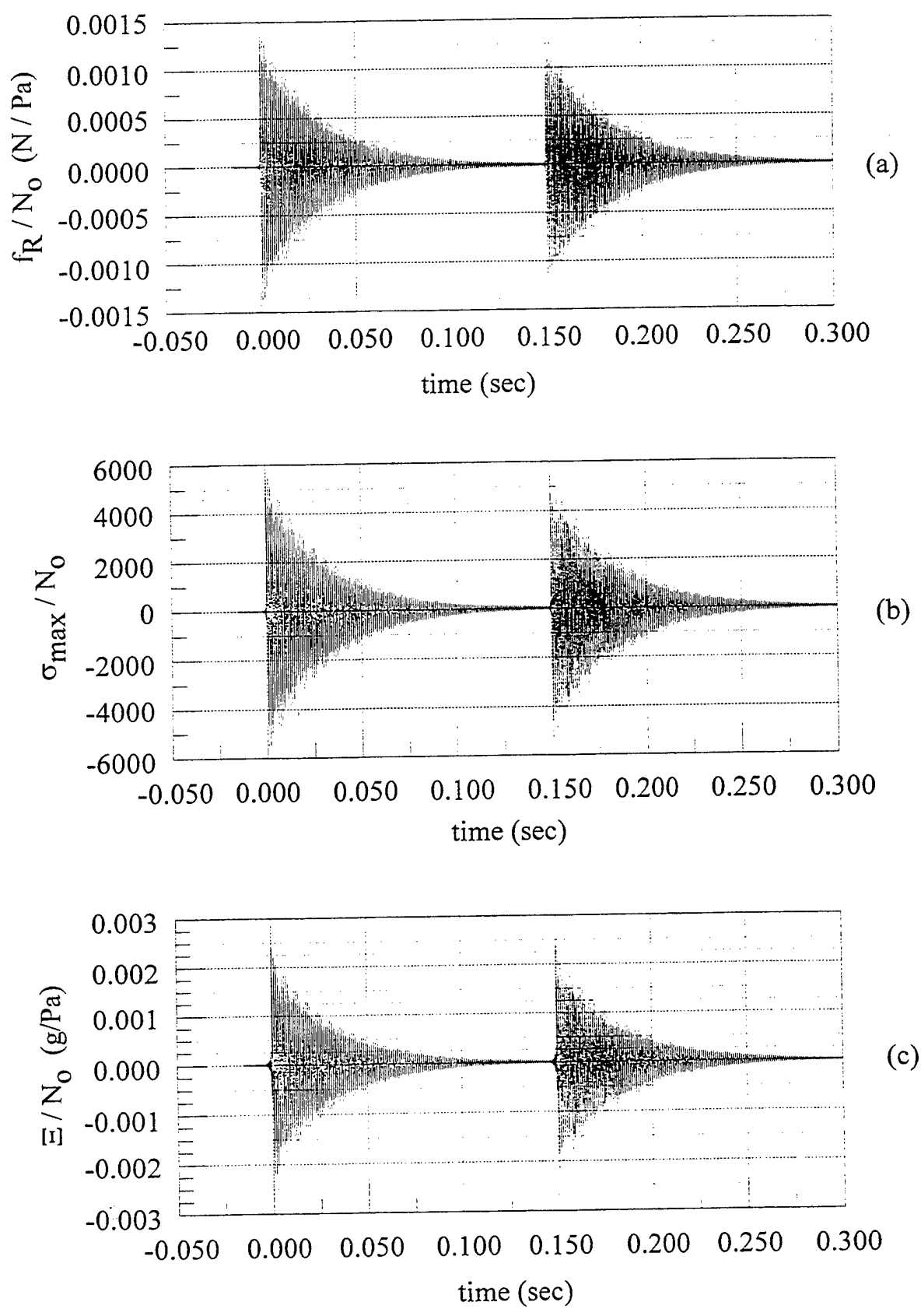


Fig. 9 Finite element interim model (pressure doubling substrate) response to unit N-wave excitation at  $\alpha=0$ . (a) reaction force (b) stress at position of peak stress (c) embryo acceleration.

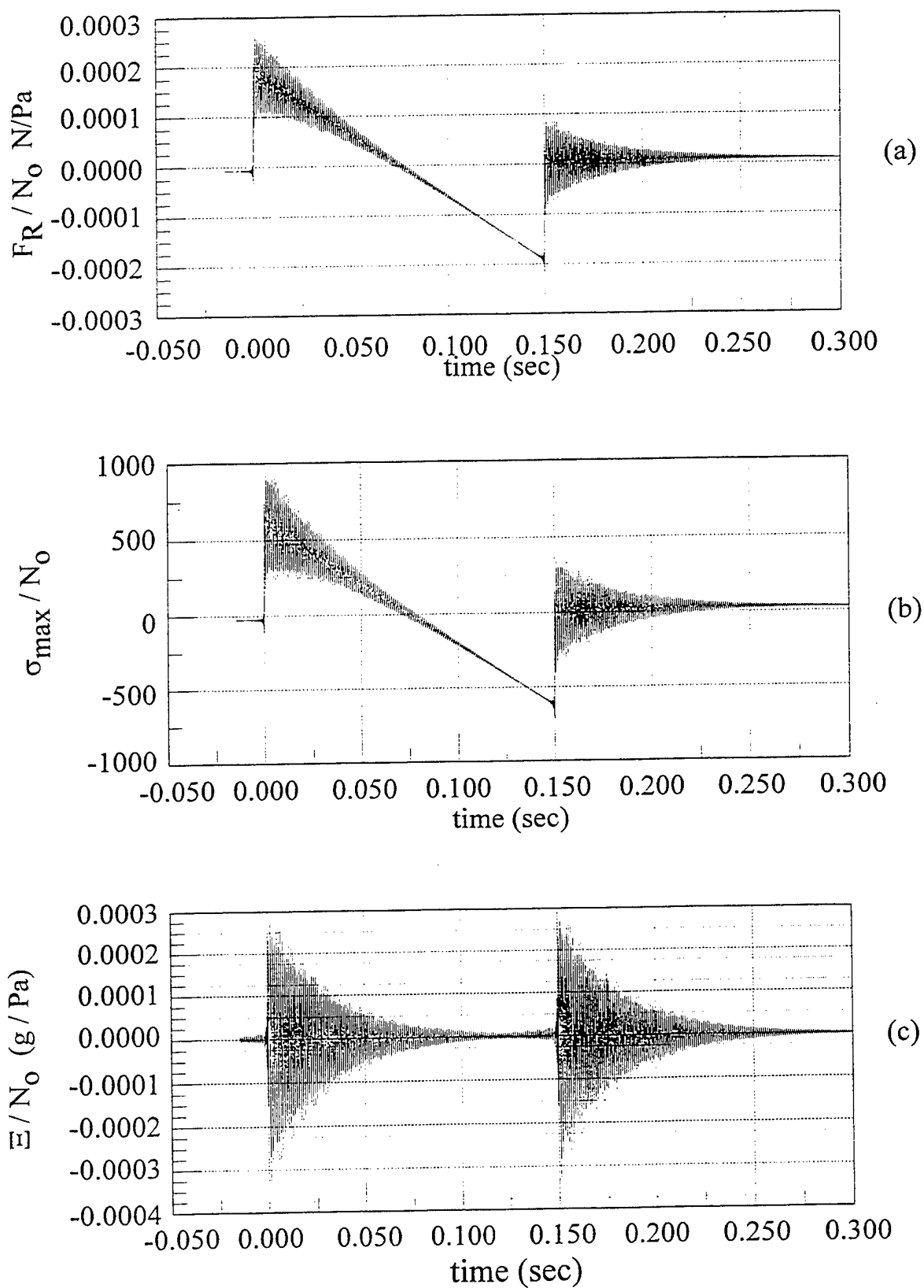


Fig. 10 Finite element model response to unit N-wave excitation at  $\alpha=0$ . (a) reaction force (b) stress at position of peak stress (c) embryo acceleration.

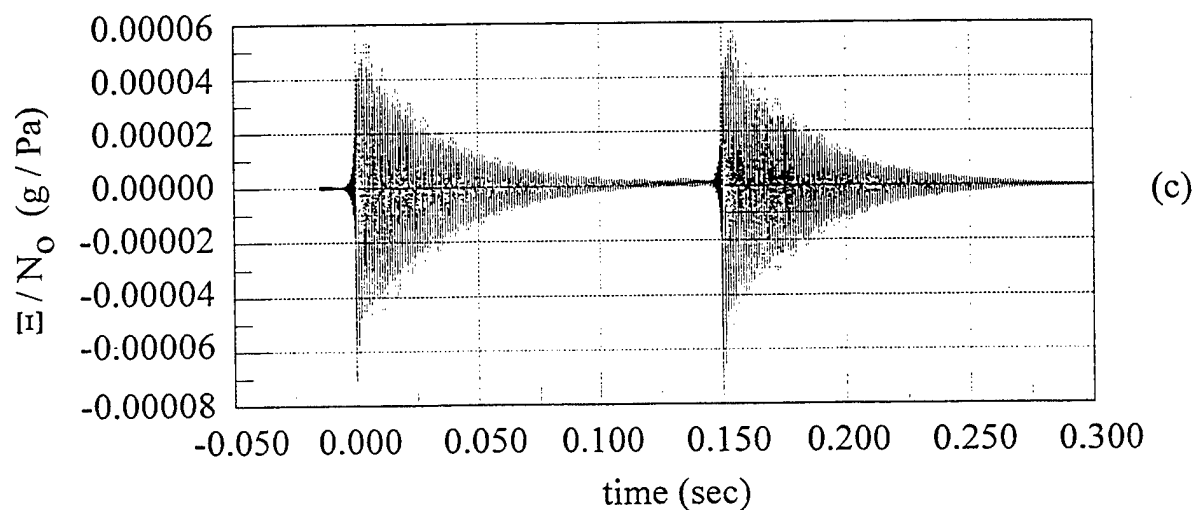
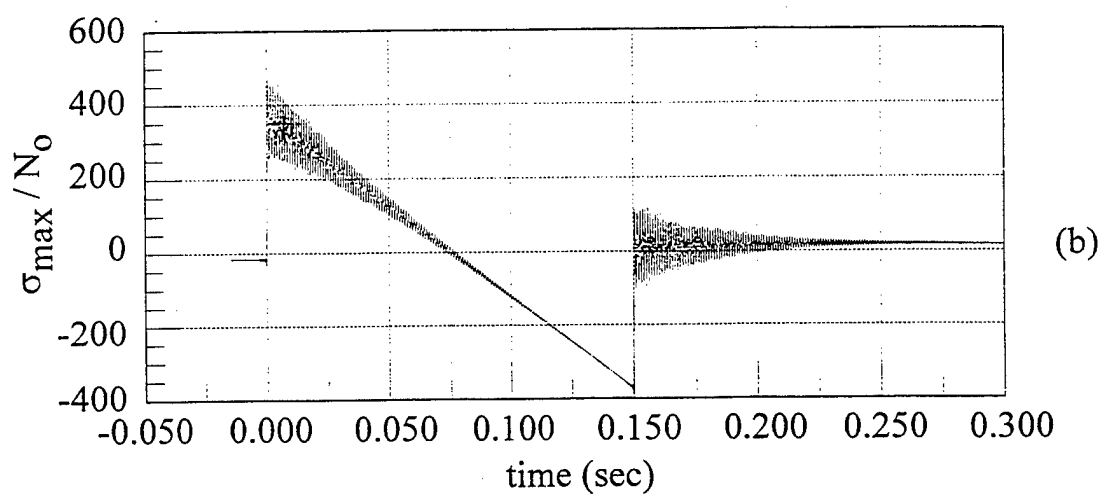
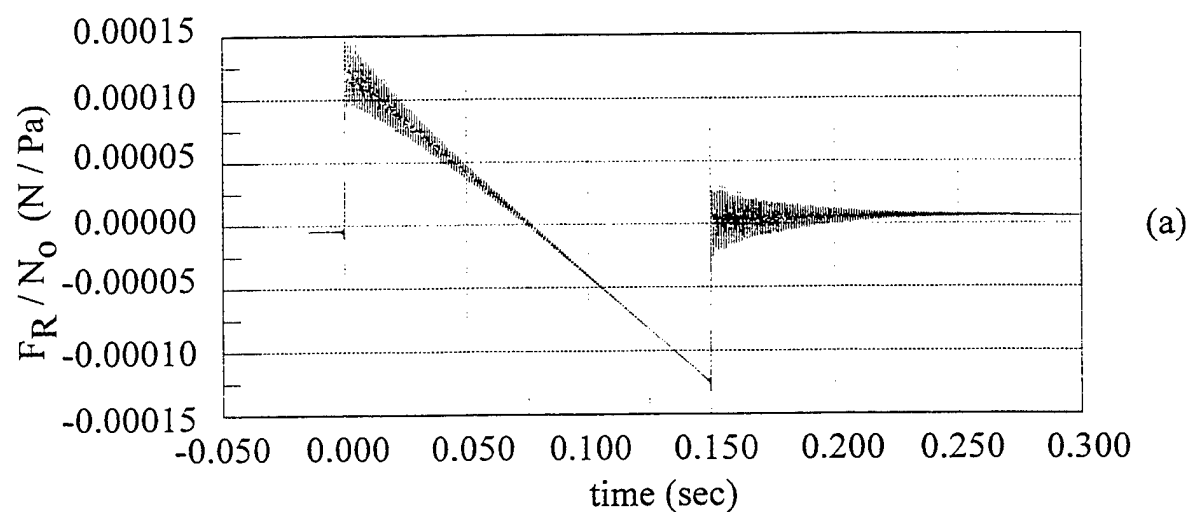


Fig. 11 Finite element model response to unit N-wave excitation  $\alpha=56^\circ$ . (a) reaction force (b) stress at position of peak stress (c) embryo acceleration.

This page intentionally left blank.



APPENDIX A: ULTRASOUND MEASUREMENT OF  
EGG SHELL PROPERTIES

**INTRASCAN**  
Daniel J. Cotter  
6 Pleasant Street  
Easton, MA 02356  
(508)238-9127

11/24/96

Joel M. Garrelick  
Kyle Martini  
Cambridge Acoustical Associates, Inc.  
200 Boston Avenue, Suite 2500  
Medford, MA 02155-4243

Dear Gentlemen:

The acoustic velocities of egg materials were measured employing Intrascan's Ultrasonic Materials Properties Evaluation System. A Panametric's M208, 20-MHz longitudinal wave transducer with a delay line was used. The velocity of sound was calculated for the egg white, yoke, and shell based on acquired time-of-flight data.

#### **Calibration of the Liquid Path Distance**

A simple measurement chamber was constructed utilizing a common glass vial to enable measurement of the time-of-flight for liquids. The transducer was positioned to a stop above the liquid with the delay line immersed. The distance from the end of the delay line to a reflector was measured employing the known acoustic velocity of water. The liquid path was determined to be 18.9 mm based on the acoustic velocity of water, 1.49 mm/microsecond, and the measured time-of-flight, 12.7 microseconds.

The ultrasonic pulser receiver parameters (gain, time dependent gain, voltage level, etc.) were adjusted to provide adequate signal to noise ratio, and allow ease of viewing the reflected signals. The transducer was operated in pulse-echo mode. Time-of-flight was digitally measured employing a mode three technique. Mode three measures the time-of-flight between multiple back echoes to reduce dependance on coupling and impedance mismatch of the transducer. The waveforms were displayed on a PC based oscilloscope emulator, and time selective gates were positioned to ensure discrimination of the reflections of interest.

#### **Determining the Acoustic Velocities of the Egg White and Yoke**

The time-of-flight of the egg white in the liquid path of 18.9 mm was 12.475 microseconds. This corresponds to a longitudinal wave velocity for the egg white of 1.520 mm/microsecond. The egg yolk had a time-of-flight of 12.790 microseconds for

the same liquid path, or 1.477 mm/microsecond. The water, egg white, and egg yolk were at room temperature (approximately 25°C) when the measurements were made. Care was taken to separate the egg white and yolk before pouring the materials into the vial. The egg yolk appeared to be frothy or aerated the first time it was measured. This was not apparent on subsequent measurements, where the yolk did not appear to "break".

### **Measurement of the Acoustic Velocity of the Egg Shell**

The time-of-flight of the longitudinal wave through the egg shell was measured employing the same transducer previously described in contact mode. A liquid couplant was used between the outside of the egg shell and the transducer delay line. The time-of-flight measurements were repeatable and yielded 59-60 nanoseconds. Mechanical measurements using a micrometer on a flattened shell in proximity to the acoustic evaluation site indicated 406 micrometers (0.016 inches). The calculated velocity was 6.89 mm/microsecond. This longitudinal wave velocity is higher than most metals and more comparable to porcelain or ceramic values in the Literature.

It was remarkable how repeatable the measurements were once the time selective gates and ultrasonic pulser parameters were established. The transducer could be moved about the egg shell while monitoring the digital signal. Of course, once the velocity is calibrated, the thickness gradient across the egg could be quantified. The Intrascan system can be operated as a thickness gage. The liquid and liquid level in the egg could be monitored because of the gross change in impedance of interface. The difference in reflected and transmitted pressure could be readily calculated for the air or liquid boundaries.

The wavelength of the longitudinal signal was on the order of the thickness of the shell. Ideally, the specimen should be 5 wavelengths thick. Higher frequency measurements could be made for comparison. For example, Intrascan owns and uses a Panametrics 5218 thickness gage pulser receiver with a 100 MHz bandwidth for evaluation of thin materials. The shear wave velocity could not be readily measured.

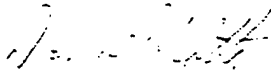
The return signal of a normal incidence shear wave transducer was not detectable. It is probable that the signal was lost in the "main bang" (excitation pulse or front surface interface). The velocity of the shear wave is typically 50% of the longitudinal wave; however, a 5-MHz normal incidence shear wave transducer was employed. Consequently, the wavelength was approximately doubled. The appropriate first critical angle for the transducer can be calculated based on the measured velocities for the shell. Additionally, higher frequency probes are commercially available. Measurement of the shear wave velocity and the calculation of the elastic properties for the egg shell were beyond the scope of the initial effort.

A three part proposal will be prepared under a separate cover.

- 1) Assessment of the feasibility of measuring the shear wave velocity, thereby enabling calculation of the elastic properties (Young's Modulus, Shear Modulus, and Poisson's Ratio) of the shell.
- 2) Assessment of the feasibility of monitoring the impact of an equivalent sonic pressure pulse (sonic boom) on the egg liquids in real-time. The compression and rarefaction of a liquid has been measured in real-time in Intrascan's laboratory. This is typically done to characterize the wavefront of pulses from transducers in water.
- 3) Quotation and description of Intrascan's system.

If you have any questions, please call.

Sincerely,



Daniel J. Cotter

APPENDIX B: MECHANICAL STRENGTH TEST RESULTS FOR  
EGGS AND EGGSHELL

Prepared by:  
Plastics Engineering Department of the  
University of Massachusetts at Lowell

(Fig. B.1)

Cambridge Acoustical  
 Summary of Test Results  
 Dec. 14, 1996  
 Page 1 of 2

Rate of extension for tests unless otherwise noted:  
 rate = 0.2 inches per minute

Egg puncture - Pressure foot area =  $0.312 \text{ cm}^2$  The load is expressed as the maximum load to first failure point. This represented the point where the shell started to crack.

Whole egg (full) - load to initial failure - pounds (kg)

7.58 (3.44)

7.46 (3.39)

7.18 (3.26)

Slope of load/compression curve:  
 "elastic region" = 1,158 lbs/inch  
 at break point = 1,371 lbs/inch  
 load rate = 0.02 IPM

Ave. 7.41 (3.36)

Blown (empty) egg shell - load to failure - pounds (kg)

9.02 (4.10)

7.90 (3.59)

3.88 (1.76)

8.82 (4.00)

6.81 (3.09)

8.85 (4.02)

5.30 (2.41)

Slope of load/compression curve:  
 "elastic region" = 769 lbs/inch  
 this value near constant over full  
 test range. load rate = 0.02 IPM

Ave. 7.23 (3.28)

Egg crush - The load is expressed as the maximum load exerted between two platens, platens larger in diameter than the egg, to first failure point. This represented the point where the shell started to crack.

Whole egg (full) - load to initial failure - pounds (kg)

6.26 (2.84)

7.34 (3.33)

6.67 (3.03)

Ave. 6.76 (3.07)

Cambridge Acoustical  
 Summary of Test Results  
 Dec. 14, 1996  
 Page 2 of 2

Hoop stress - The egg shell was sliced to form a ring around the largest diameter of the egg. The ring was tested on a fixture under tensile load. The fixture was "fitted" into the shell ring to restrict deformation of the shell during extension.

Hoop width (in):	0.477	0.472	0.476	0.472
	0.478	0.473	0.476	0.476
	0.472	0.474		

Ave. = 0.475 inches (1.207 cm)

Hoop Stress - pounds (kg) Actual load is one half the reported values listed below.

1.24 (0.565)
1.41 (0.640)
2.28 (1.035)
1.98 (0.900)
1.62 (0.734)

Ave. 1.71 (0.775)

Hoop compression - The egg shell was sliced to form a ring around the largest diameter of the egg. The ring was tested between two flat platens under a compression load. The egg shell was placed on a small dab of plaster of paris to prevent the ring from slipping during test. The shell ring to free to deform during compression.

Hoop width (in):	0.471	0.476	0.476	0.473
	0.472	0.477	0.472	0.473
	0.476	0.474	0.476	0.472
	0.476	0.475	0.474	0.475
	0.474	0.477		

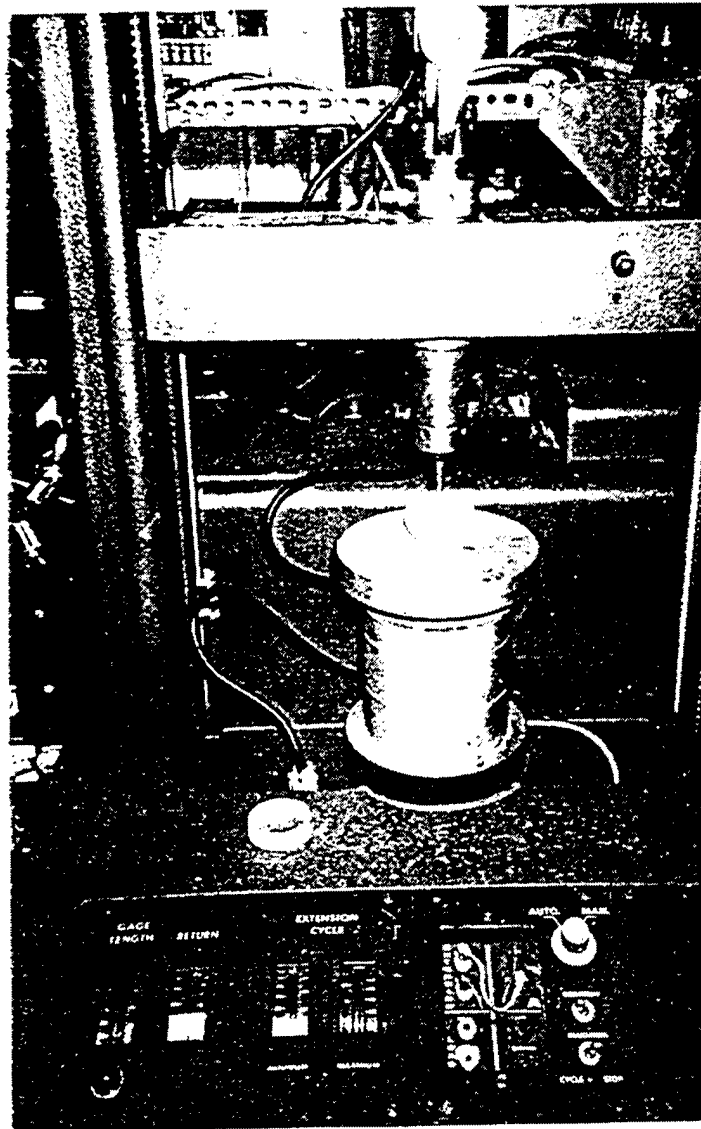
Ave. = 0.474 inches (1.204 cm)

Hoop compression - pounds (kg) - "Elastic" slope lb/inch

#T	0.339 (0.154)	0.754
#1	0.293 (0.133)	0.692
#2	0.229 (0.104)	0.416
#3	0.326 (0.148)	0.753
#4	0.282 (0.128)	0.661
#5	0.313 (0.142)	0.759
Ave.	0.297 (0.135)	0.673

Fig. B.1 Egg strength testing apparatus.

(a) Sample Configuration For Measuring Egg Failure Load



(b) Sample Configuration For Measuring Egg Shell Failure Stress

